Inelastic light scattering at metal–insulator transition: ripple and elasto-optic mechanisms

L. A. Falkovsky and E. G. Mishchenko
Institute for Theoretical Physics L. D. Landau RAS 117334 Moscow, Russia

(Submitted 20 March 1995)
Pis'ma Zh. Éksp. Teor. Fiz. **61**, No. 8, 678–683 (25 April 1995)

The inelastic light scattering in metals and insulators by acoustic and optical phonons is considered. The ripple and elasto-optic mechanism are taken into account. The phonon damping and skin effect are analyzed. The surface contribution to the cross section is found to be insensitive to the skin depth. The influence of the carriers on the bulk contribution through the skin effect and through the phonon damping is essential. The recent experimental data for fullerides are discussed.

1. The inelastic light scattering is a widespread experimental tool in investigating phonon spectra of various systems.[1–3] But despite the large number of papers devoted to the subject the theory is still far from complete. The surface effects seems to be an important problem. Although their significance was recognized for a long time, a thorough description has not been given until now.

Several papers contain the theory of Brillouin scattering from acoustic phonons in insulators in more or less transparent manner for different models, in which the presence of a surface is taken into account.[4–7] On the other hand, the inelastic light scattering by phonons in metals has been investigated less extensively. A few attempts[8,9] devoted to Raman scattering, which used the Green's function formalism, had failed to consider the surface of a sample. The theory of Brillouin scattering in metals appears to have been proposed first by the present authors,[10,11] using a straightforward semiclassical approach. A similar theory for the Raman light scattering from optical phonons was also presented in Ref. 12.

Our main purpose is to compare the inelastic light scattering from phonons in metals and insulators. Since the skin depth in metals is small, we must take into account the scattering by the movement on the surface (ripples). The surface contribution from the ordinary elasto-optic mechanism should also be included.

Let us consider an incident light wave with a frequency $\omega^{(i)}$, which propagates normal to the surface (along the z axis), and a light wave with a frequency $\omega^{(s)}$ scattered in the xz plane. If $\omega^{(i)}$ and $\omega^{(s)}$ are in the normal skin range and the polarizations are perpendicular to the xz plain, the spatial distribution of the field in the metal is determined by the z component of the wave vectors:

$$\zeta^{(i,s)}=(\epsilon(\omega^{(i,s)})\omega^{(i,s)2}/c^2-k_s^{(i,s)2})^{1/2}.$$

There are two mechanisms of light scattering in metal. One (elasto-optic) mechanism, which is associated with the electronic density fluctuations, has the following cross section:[13]

$$\frac{d^2\sigma_{el}}{d\omega^{(s)}do^{(s)}}=\frac{(\omega_P/\omega^{(i)})^4}{2\pi^3c^5}\frac{k_z^{(i)}k_z^{(s)2}\omega^{(i)3}\omega^{(s)2}}{|k_z^{(i)}+\zeta^{(i)}|^2|k_z^{(s)}+\zeta^{(s)}|^2}\times\int_0^\infty\int_0^\infty dz\,dz'U(z)U^*(z')$$
$$\times\langle\langle\delta n_\gamma(z,\mathbf{k}_s,\omega)\delta n_{\gamma*}(z',\mathbf{k}_s,\omega)\rangle\rangle. \tag{1}$$

Here $\omega_P^2=4\pi e^2n_e/m$, where n_e is the density of electrons. The vector components $\mathbf{k}_s$ are along the surface, and $k_z^{(i)}$ and $k_z^{(s)}$ are the normal components of the wave vectors for the incident and scattered light in the vacuum. We introduce the frequency and momentum transfer $\omega=\omega^{(i)}-\omega^{(s)}$ and $\mathbf{k}_s=\mathbf{k}_s^{(i)}-\mathbf{k}_s^{(s)}$. For the considered geometry we have $\mathbf{k}_s^{(i)}=0$. The operator δn_γ can be expressed in terms of the electronic distribution function $\delta f_p(\mathbf{r},t)$:

$$\delta n_\gamma(\mathbf{r},t)=\frac{2}{n_e}\int\frac{d^3p}{(2\pi)^3}\gamma_{yy}(\mathbf{p})\delta f_p(\mathbf{r},t) \tag{2}$$

and the effective electron-photon vertex

$$\gamma_{\alpha\beta}(\mathbf{p})=\delta_{\alpha\beta}+\frac{1}{m}\sum_n\left(\frac{p_{fn}^\alpha p_{nf}^\beta}{\varepsilon_{fn}(\mathbf{p})+\omega^{(i)}}+\frac{p_{fn}^\beta p_{nf}^\alpha}{\varepsilon_{fn}(\mathbf{p})-\omega^{(s)}}\right), \tag{3}$$

where the sum is taken over all zones n. The subscript f denotes the conduction band, $\varepsilon_{fn}=\varepsilon_f-\varepsilon_n$. The factor $U(z)=\exp(i\zeta_1z-\zeta_2z)$ describes the penetration of light into the crystal, where the complex quantity $\zeta_1+i\zeta_2=\zeta^{(i)}+\zeta^{(s)}$.

The ripple contribution is given by the electromagnetic boundary conditions at the surface which move due to phonons. As a result, the inelastic light scattering becomes possible without any elasto-optic interaction. The scattering cross section by ripples has the form

$$\frac{d^2\sigma_{\text{rip}}}{d\omega^{(s)}do^{(s)}}=\frac{|\epsilon_{yy}(\omega^{(i)})-1|^2}{2\pi^3c^5}\frac{k_z^{(i)}k_z^{(s)2}\omega^{(i)3}\omega^{(s)2}}{|k_z^{(i)}+\zeta^{(i)}|^2|k_z^{(s)}+\zeta^{(s)}|^2}\langle\langle u_z^{\text{sur}}(\mathbf{k}_s,\omega)u_z^{\text{sur}*}(\mathbf{k}_s,\omega)\rangle\rangle. \tag{4}$$

Here u_z^{sur} denotes the surface displacement. The connection of u_z^{sur} with the acoustic $u(\mathbf{r},t)$ and the optical $w(\mathbf{r},t)$ phonon displacements is determined by the surface orientation with respect to the crystal axes. The result is expressed in terms of the correlators $\langle\langle u_z(\mathbf{s},z=0,t)u_z(\mathbf{s},z=0,t)\rangle\rangle$ and $\langle\langle w_z(\mathbf{s},z=0,t)w_z(\mathbf{s},z=0,t)\rangle\rangle$, where the statistical average is taken.

2. The correlators (1) and (4) were evaluated in our recent papers[10–13] with the help of the fluctuation-dissipation theorem, the Boltzmann equation, and the equation of the dynamic theory of elasticity.[14] The following notation used:

$$\frac{\left\{\begin{array}{l}\sum_{\text{el}}(\mathbf{k}_s,\omega)\\ \sum_{\text{rip}}(\mathbf{k}_s,\omega)\end{array}\right.}{1-\exp(-\omega/T)}=\left\{\begin{array}{l}\int_0^\infty\int_0^\infty dz\,dz'U(z)U^*(z')\langle\langle\delta n_\gamma(z,\mathbf{k}_s,\omega)\delta n_{\gamma*}(z',\mathbf{k}_s,\omega)\rangle\rangle\\ |\epsilon(\omega^{(i)})-1|^2\langle\langle u_z^{\text{sur}}(\mathbf{k}_s,\omega)u_z^{\text{sur}*}(\mathbf{k}_s,\omega)\rangle\rangle.\end{array}\right. \tag{5}$$

Both the elasto-optic and ripple mechanisms have the same resonant factors at the frequency of the interband transition, since γ_{yy} (3), and the dielectric function ϵ_{yy} have the same singularities. For example, in a Drude–Lorentz model we have

$$\epsilon(\omega^{(i)})\simeq 1-\frac{\omega_p^2}{\omega^{(i)2}}+\sum_n\frac{\Omega_n^2}{\varepsilon_{fn}^2-\omega^{(i)2}}. \tag{6}$$

In the following discussion we omit these resonant factors.

The correlator Σ_{rip} for an isotropic crystal has the form

$$\sum_{\text{rip}}(\mathbf{k}_s,\omega)=\frac{1}{\rho\omega^2}\,\text{Im}\left(\frac{k_s^2}{\kappa_t}-\kappa_l-\frac{\omega^4\kappa_l/s_t^4}{(k_s^2+\kappa_t^2)^2-4k_s^2\kappa_l\kappa_t}\right), \tag{7}$$

where ρ is the crystal density, κ_l and κ_t describe the z dependence of the longitudinal and transverse mode amplitude: The real κ indicates the mode that decays in the bulk. The correlator Σ_{el} contains the contributions from electron-hole excitations and from optical and acoustic phonons via the electron-phonon interaction.[10–13,15] We consider only the phonon contributions.

Let us initially consider the Brillouin scattering, i.e., the scattering with excitation or absorption of acoustic phonons (Fig. 1). For acoustic phonons we have $\kappa_{l,t}^{ac}=(k_s^2-\omega^2/s_{l,t}^2)^{1/2}$, where s_l and s_t are the longitudinal and transverse sound velocities. In the range $\omega<s_tk_s$ the imaginary part in (7) arises only from the third term and its peak is related to the Rayleigh wave (the same peak appears in the elasto-optic contribution):

$$\left.\begin{array}{l}\sum\limits_{\text{el}}^{\text{ac}}(\mathbf{k}_s,\omega)\\ \sum\limits_{\text{rip}}^{\text{ac}}(\mathbf{k}_s,\omega)\end{array}\right\}\simeq\frac{\Gamma_{\text{ac}}}{\rho s[(\omega-s_Rk_s)^2+\Gamma_{\text{ac}}^2]}, \tag{8}$$

where s_R is the Rayleigh wave velocity. The acoustic phonon damping includes the contribution from the electron-phonon interaction:

$$\Gamma_{\text{ac}}(\mathbf{k})=\frac{k^2}{2\rho}\,\text{Im}\int\left\langle\frac{\lambda^2(\mathbf{p})}{\mathbf{vk}-i\tau_p^{-1}}\right\rangle\frac{dS_F}{v(2\pi)^3}, \tag{9}$$

where $\lambda(\mathbf{p})$ is the deformation potential, and τ_p^{-1} is the electron collision rate; the integral is taken over the Fermi surface. For small carrier concentration n, Γ_{ac} is proportional to n, since the average of λ over the Fermi surface is equal to zero. We see from (8) that

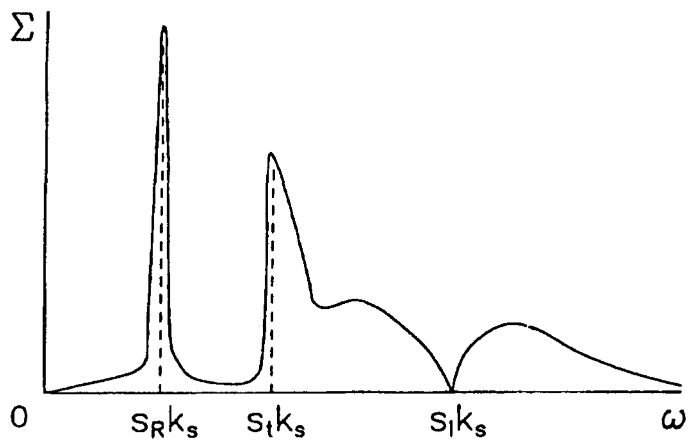

FIG. 1. Cross section for the ripple Brillouin scattering. The left peak at $\omega=s_R k_s$ is associated with the Rayleigh wave (8). The nonsymmetric maximum near $\omega=s_t k_s$ is related to the transverse phonon slipping along the surface. The continuum between $\omega=s_t k_s$ and $\omega=s_l k_s$ involves the "mixed"-phonon mode. The right continuum at $\omega>s_l k_s$ follows from the bulk phonons which are reflected from the surface.

the elasto-optic mechanism and the ripple mechanism give similar contributions which are virtually independent of the skin depth. This result contradicts the result reported in Ref. 7.

In the domain $s_t k_s<\omega<s_l k_s$ the narrow continuum associated with the "mixed" mode (with decaying longitudinal wave and nondecaying transverse wave) appears in the electronic and the ripple cross section:

$$\left.\begin{array}{l}\sum\limits_{\mathrm{el}}^{\mathrm{ac}}(\mathbf{k}_s,\omega)\\ \sum\limits_{\mathrm{rip}}^{\mathrm{ac}}(\mathbf{k}_s,\omega)\end{array}\right\}\simeq(s_l^2k_s^2-\omega^2)(\omega^2-s_t^2k_s^2)^{1/2}/\rho s^5k_s^4. \tag{10}$$

The first term in (7) gives the additional ripple contribution (asymmetric transverse resonance) which is absent in Σ_{el}:

$$\sum_{\mathrm{rip}}^{\mathrm{ac}}(\mathbf{k}_s,\omega)\simeq\frac{s_tk_s^2}{\rho\omega^2}\,\mathrm{Re}(\omega^2-s_t^2k_s^2+2i\Gamma_{\mathrm{ac}}\omega)^{-1/2}. \tag{11}$$

It is produced by transverse phonons which slip along the surface. Finally, in the range $\omega>s_l k_s$ we have a wide asymmetric longitudinal resonance due to the electron-phonon interaction and the continuum by the ripples:

$$\left.\begin{array}{l}\sum\limits_{\mathrm{el}}^{\mathrm{ac}}(\mathbf{k}_s,\omega)\\ \sum\limits_{\mathrm{rip}}^{\mathrm{ac}}(\mathbf{k}_s,\omega)\end{array}\right\}\simeq\left\{\begin{array}{l}\dfrac{s_l k_s^4}{\rho\omega^2(\zeta_1^2+\zeta_2^2)}\,\mathrm{Re}(\omega^2-s_l^2k_s^2+2i\Gamma_{\mathrm{ac}}\omega)^{-1/2},\\ (\omega^2-s_l^2k_s^2)^{1/2}/\rho s\omega^2.\end{array}\right. \tag{12}$$

The first and second terms in the brackets (7) are absent in Refs. 6 and 7. We derive them from the "bulk" part of the phonon Green's function. The last term in (7) arises from the "surface" part. The entire Green's function obeys the elastic equation for the semi-space $z>0$ and the boundary condition at $z=0$.

The elasto-optic cross section also contains the contribution from bulk phonons. For the normal incidence and scattering only the longitudinal phonons are involved. The corresponding peak is sharp when the skin depth is small, $\zeta_1 \gg \zeta_2$:

$$\sum_{\mathrm{el}}^{\mathrm{ac}}(\mathbf{k}_s,\omega)\simeq\left\{\begin{array}{ll}\dfrac{\zeta_1}{\rho[(\omega-s_l\zeta_1)^2+s_l^2\zeta_2^2]} & \text{for } s_l\zeta_2\gg\Gamma_{\mathrm{ac}},\\ \dfrac{\zeta_1\Gamma_{\mathrm{ac}}}{\rho s_l\zeta_2[(\omega-s_l\zeta_1)^2+\Gamma_{\mathrm{ac}}^2]} & \text{for } s_l\zeta_2\ll\Gamma_{\mathrm{ac}}.\end{array}\right. \tag{13}$$

For the nonperpendicular incidence and scattering the bulk transverse phonons are excited, giving the peak with the same form (13) multiplied on $\min(k_s^2/\zeta_1^2,\zeta_1^2/k_s^2)$.

3. The Raman scattering of light from optical phonons can be analyzed similarly. To find the optical part of the correlator (4) we apply the elasto-optic equation taking into account the electron–optical-phonon interaction.[11,12] After the evaluation we obtain expression (7) with $\kappa_{l,t}^{\mathrm{op}}=(k_s^2-(\omega^2-\omega_{l,t}^2)/a_{l,t})^{1/2}$. Here $\omega_{l,t}$ and $a_{l,t}$ define the bulk optical spectrum $\omega_{l,t}(k)^2=\omega_{l,t}^2+a_{l,t}k^2$. The dispersion parameters $a_{l,t}$ are on the order of s^2 and may have an arbitrary sign. The surface optical phonons exist when κ_l^{op} and κ_l^{op} are both real. In contrast with the acoustic case, there are two branches of the optical surface phonons[12] for the case of two atoms in a unit cell. Each of them produces a strong Lorentzian peak:

$$\left.\begin{array}{l}\sum\limits_{\mathrm{el}}^{\mathrm{op}}(\mathbf{k}_s,\omega)\\ \sum\limits_{\mathrm{rip}}^{\mathrm{op}}(\mathbf{k}_s,\omega)\end{array}\right\}\simeq\frac{\Gamma_{\mathrm{op}}}{\rho s((|\omega|-\omega_s(k_s))^2+\Gamma_{\mathrm{op}}^2)}\left\{\begin{array}{c}\min(p_F^2/|\zeta|^2,p_F^2/k_s^2)\\ 1\end{array}\right., \tag{14}$$

where $\omega_s(k_s)$ are their spectra. The optical phonon damping was evaluated self-consistently[12] and has the form

$$\Gamma_{\mathrm{op}}(\mathbf{k})=-\frac{1}{2\rho}\,\mathrm{Im}\int\left\langle\frac{\xi^2(\mathbf{p})}{\omega-\mathbf{vk}+i\tau_p^{-1}}\right\rangle\frac{dS_F}{v(2\pi)^3}, \tag{15}$$

where $\xi(\mathbf{p})$ is the optical deformation potential. The electron-phonon interaction gives the optical frequency shift

$$\delta\omega=\frac{1}{2\rho\omega}\,\mathrm{Re}\int\frac{(i\tau_p^{-1}-\mathbf{vk})\xi^2(\mathbf{p})}{\omega-\mathbf{vk}+i\tau_p^{-1}}\,\frac{dS_F}{v(2\pi)^3}. \tag{16}$$

The various asymmetric resonances and continua appear near the frequencies which obey the condition $\kappa_l=0$ or $\kappa_t=0$. The detailed analysis is rather sophisticated and depends on the relations of the spectrum parameters.

The optical bulk peaks arise only in the elasto-optic contribution. For example, the shape of the longitudinal phonon peak has the form

$$\sum_{\mathrm{el}}^{\mathrm{op}})\mathbf{k}_s,\omega)\simeq\begin{cases}\dfrac{p_F\Gamma_{\mathrm{op}}}{\rho s\zeta_2[(\omega-(\omega_l^2+a_l\zeta_1^2)^{1/2})^2+\Gamma_{\mathrm{op}}^2]} & \text{for } s\zeta_2\ll\Gamma_{\mathrm{op}}p_F/\zeta_1,\\ \dfrac{p_F^2}{\rho\zeta_1[(\omega-(\omega_l^2+a_l\zeta_1^2)^{1/2})^2+s_l^2\zeta_2^2]} & \text{for } s\zeta_2\gg\Gamma_{\mathrm{op}}p_F/\zeta_1.\end{cases} \quad (17)$$

In the last case, when $s\zeta_2\gg\Gamma_{\mathrm{op}}p_F/\zeta_1$, an additional peak controlled by the singularity of the phonon density of states appears:

$$\sum_{\mathrm{el}}^{\mathrm{op}}(\mathbf{k}_s,\omega)\simeq\frac{p_F^2}{\rho s(\zeta_1^2+\zeta_2^2)}\,\mathrm{Re}(\omega^2-\omega_l^2+2i\Gamma_{\mathrm{op}}\omega_t)^{-1/2}. \quad (18)$$

This peak has an asymmetric shape. Its symmetry changes simultaneously with the sign of a.

4. In the experiments the incident light frequency is usually used in the transparency range to increase the penetration depth. Now let us imagine that the number of carriers increases in a sample. The experimental results on fullerides[16] show that most of the vibrational modes disappear for the metallic phase A_3C_{60} in comparison with the Raman spectra for the insulator phases C_{60} and A_6C_{60}. Two explanations for this phenomenon can be proposed. The first one suggests the strong influence of carriers on the skin depth: The doping can render the dielectric function (6) negative at incident or scattered frequency. In this case $\zeta_2\sim\zeta_1$ and all the bulk peaks [(13), (17), and (18)] become unobservable. The acoustic surface resonances (8)–(12) and the optical surface resonances still exist.

The alternative explanation involves the effect of carriers on the phonon damping. As we can see from (9), (15), and (16), the interaction of carriers with phonons causes the broadening and the shift of the peaks. The electron-phonon damping can be forbidden by selection rules. For example, if the optical phonon polarization is perpendicular to the vector of the deformation potential, the damping and shift are equal to zero, (15) and (16). Indeed, the experimental data demonstrate the broadening and shift of most peaks. Complementary data to the Raman studies come from inelastic neutron scattering. Here the skin depth should not affect the neutron spectra. In our view, a scenario cannot be chosen from the data of Ref. 17.

L.A.F. is grateful to I. Luk'yanchuk for a discussion of the properties of fullerides. E.G.M. thanks KFA, Forshchungszentrum, Jülich, Germany for financial support. This work was supported by the Russian Foundation for Fundamental Research.

[1] J. R. Sandercock, Solid State Commun. **26**, 547 (1978).
[2] F. Nizoli and J. Sandercock, in *Dynamical Properties of Solids*, edit. by G. K. Horton and A. A. Maradudin, North-Holland, Amsterdam **6**, 281 (1990).

[3]V. V. Aleksandrov, T. S. Velichkina, P. G. Vorob'ev *et al.*, Zh. Éxp. Teor. Fiz. **103**, 2170 (1993) [JETP **76**, 1085 (1993)].
[4]D. L. Mills, Phys. Rev. B **15**, 2097 (1977).
[5]K. R. Subbaswamy and A. A. Maradudin, Phys. Rev. B **18**, 4181 (1978).
[6]R. Loudon, Phys. Rev. Lett. **40**, 581 (1978).
[7]A. M. Marvin, V. Bortolani, and Nizzoli, J. Phys. C: Solid St. Phys. **13**, 299 (1980).
[8]K. Itai, Phys. Rev. B **45**, 707 (1992).
[9]V. N. Kostur, Z. Phys. B **89**, 142 (1992).
[10]L. A. Falkovsky and E. G. Mishchenko, Pis'ma Zh. Éxp. Teor. Fiz. **59**, 687 (1994) [JETP Lett. **59**, 726 (1994)].
[11]L. A. Falkovsky and E. G. Mishchenko, Phys. Rev. B **51** (1995).
[12]E. G. Mishchenko and L. A. Falkovsky, Zh. Éxp. Teor. Fiz. **107**, 936 (1995) [JETP **80**, 531 (1995)].
[13]L. A. Falkovsky and S. Klama, Phys. Rev. B **50**, 5666 (1994).
[14]V. M. Kontorovich, Usp. Fiz. Nauk **142**, 265 (1984).
[15]A. Zawadowski and M. Cardona, Phys. Rev. B **42**, 10732 (1990).
[16]S. J. Duclos, R. C. Haddon, S. Glarum *et al.*, Science **254**, 1625 (1991).
[17]K. Prassides, J. Tomkinson, C. Christides *et al.*, Nature **354**, 462 (1991).

Published in English in the original Russian journal. Reproduced here with stylistic changes by the Translation Editor.